# Pharmacokinetic–pharmacodynamic modelling of human insulin: validity of pharmacological availability as a substitute for extent of bioavailability

Makoto Miyazaki, Haruko Mukai, Kazunori Iwanaga, Kazuhiro Morimoto and Masawo Kakemi

## Abstract

A method for assessing the extent of bioavailability (EBA) of human insulin from pharmacological data was determined. The time course governing increases in the plasma concentration of immuno-reactive insulin (IRI), as well as its pharmacological effects (gluco-dynamics), was determined after the intravascular administration of varying doses of human insulin. Pharmacokinetic (PK), pharmacodynamic (PD), and link models were constructed to elucidate the quantitative relationship between plasma IRI levels and pharmacological effects. After extravascular administration of the test formulation, only the time course governing the observed pharmacological effects was determined. The pharmacological data was translated into theoretical plasma concentration data, using the PK–PD model. Following this, the area under the theoretical plasma concentration–time curve (AUC) of the test formulation was calculated. The EBA was then estimated against a reference (intravascular) formulation, using a conventional equation. Since the pharmacological effects of insulin were observed to be highly dosing-rate-dependent, the PD model used in this study was modified to apply over a wide range of infusion rates. The results of the PK–PD analysis indicate that the doses administered can be accurately predicted from pharmacological data. To validate this method, the EBAs of controlled release formulations (the Osmotic Mini Pumps) of insulin, subcutaneously administered to the rat, were estimated. The EBA values obtained (92–96 %) fell within a reasonable range. The area under the effect–time curves (AUE) obtained following subcutaneous applications of the Osmotic Mini Pump were calculated in a model-independent manner, in addition to pharmacological availabilities (PA), which were estimated against the reference (intravascular) formulations. The estimated PA values varied from 312 % to 78 %, in accordance with the intravascular input rates of the reference formulations. This indicates that PA should not be used as a substitute for EBA, unless data involving similar intravascular dosing rates to that of the reference formulations is available.

Department of Pharmaceutics, Osaka University of Pharmaceutical Sciences, 4-20-1 Nasahara, Takatsuki, Osaka 569-1094, Japan

Makoto Miyazaki, Haruko Mukai, Kazunori Iwanaga, Masawo Kakemi

Department of Pharmaceutics, Hokkaido College of Pharmacy, 7-1 Katsuraoka-cho, Otaru, Hokkaido 047-0264, Japan

Kazuhiro Morimoto

Correspondence: M. Kakemi, Department of Pharmaceutics, Osaka University of Pharmaceutical Sciences, 4-20-1 Nasahara, Takatsuki, Osaka 569-1094, Japan. E-mail: kakemi@gly.oups.ac.jp

## Introduction

Extent of bioavailability (EBA) is one of the most important indexes in evaluating the therapeutic activity of a drug. EBA is defined as the fraction of extravascularly administered dose that reaches the systemic circulation. Since the area under the plasma drug concentration versus time curve (AUC) reflects the total amount of drug reaching the systemic circulation, oral bioavailability ($EBA_{po}$) can be determined by comparing dose-normalized AUCs after oral (extravascular) and

intravascular administration. Recently, many endogenous peptides have been developed for clinical use. These drugs regulate endocrine and other physiological processes in the body, and exert their pharmacological effects even at very low doses. Since these drugs are eliminated rapidly from the systemic circulation, determination of the plasma concentrations of these drugs is often difficult. In such situations, pharmacological availability (PA) is used empirically as a substitute for EBA.

The area under the pharmacological activity versus time curve (AUE) is a cumulative measure of overall drug activity and is known to relate, whether linearly or nonlinearly, to the free fraction of drug reaching the site of action. The PA of a drug is usually determined by comparing dose-normalized AUEs after extravascular and intravascular administration. However, a number of reports indicate that the AUE is not always proportional to the AUC (Wald et al 1991; Tachibana 1992; Derendorf 1994). Therefore, the use of PA in evaluating drug formulations might lead to erroneous conclusions (Hochhaus & Derendorf 1995). We previously presented a novel pharmacokinetic (PK)–pharmacodynamic (PD) method for assessing the EBA from pharmacological data after oral administration (Miyazaki et al 2000a, b), in which we suggested that the method is useful for evaluating the EBA of several drugs with potent pharmacological effects. The objective of this study was to investigate the applicability of our previous method to human insulin, another model compound for bioactive peptide. We also assessed the validity of PA as a substitute for EBA.

## Materials and Methods

### Chemicals

Human recombinant insulin was purchased from Becton Dickinson and Company (Franklin Lakes, NJ). Saline was obtained from Otsuka Pharmaceuticals Ltd (Tokyo, Japan). All other reagents and solvents were commercial products of reagent grade (Wako Pure Chemical Industries, Osaka, Japan).

### Animal surgery

Male Wistar rats (Japan SLC Inc., Shizuoka, Japan), 240–260 g, were used. The rats were housed in environmentally regulated facilities (temperature, $24 \pm 1°C$; humidity, $55 \pm 10\%$), in a 12-h light–dark cycle for over 1 week, and were allowed free access to a standard diet and tap water. On the day before the experiment, the rats were lightly anaesthetized with ethyl ether, and

were implanted surgically with a combination of Phicon (Fuji systems Ltd, Tokyo, Japan) and PE50 (Clay Adams, Parsippany, NJ) in a catheter, which was inserted into the right femoral vein for drug administration. Another Phicon–PE50 catheter was inserted in the right jugular vein for blood sampling. Both catheters were externalized through the back of the neck and secured. All of these methods had previously been approved by the Animal Experimentation Committee of Osaka University of Pharmaceutical Sciences.

### Animal experiments

On the day of the experiment, the rats were housed in individual metabolic cages and left for at least 1 h. Insulin was dissolved in an isotonic phosphate buffer (pH 7.4) and was infused into the femoral veins via the catheters at doses in the range 0.2–5 IU kg$^{-1}$, for 60, 120 and 180 min. In the subcutaneous administration study, an Osmotic Mini Pump (Alzet Osmotic Pump 2001, Alza Corporation, Palo Alto, CA) was used. Briefly, insulin was dissolved in saline, and injected into the Osmotic Mini Pump with a microsyringe. The rats were lightly anaesthetized with ethyl ether, and implanted surgically with the Osmotic Mini Pump in the back region. Previously, the release rate of insulin from the Osmotic Mini Pump was determined in an in-vitro study carried out at 37°C in an isotonic phosphate buffer (pH 7.4). The release (dosing) rates of insulin from the Osmotic Mini Pump were set at 5 or 10 IU kg$^{-1}$ per day. Blood samples (0.2 mL) were withdrawn from the jugular vein at predose (blank plasma), and at designated postdose intervals. The blood samples were transferred into heparinized tubes, and then centrifuged (10 000 rev min$^{-1}$ for 5 min). The isolated plasma was frozen and stored at $-20°C$ until analysis. After dilution of the plasma sample with 0.05 mol L$^{-1}$ phosphate buffer (pH 7.4), immuno-reactive insulin (IRI) levels within the plasma were determined by radio-immunoassay (Shionoria Insulin, Shionogi & Co. Ltd, Osaka, Japan). Plasma glucose concentrations were determined using the glucose oxidase method (Glucose C Test Wako, Wako Pure Chemical Industries, Osaka, Japan). The basal glucose level within the plasma was taken to be the average of data taken 60, 30 and 10 min before drug administration.

### Data analysis

The concentration–time data was analysed by a non-linear regression program, FKDM (Lu et al 1987) using a PC/AT compatible personal computer (Gateway,

North Sioux City, SD). The differential equations were solved by the Runge–Kutta–Gill method. Unless otherwise specified, AUCs were calculated to include the last measurement of concentration–time data by the linear trapezoidal method, and AUCs extending beyond the last data sampling point were estimated by dividing the final concentration–time data by the terminal slope. AUEs following the intravascular or extravascular administration of insulin were also calculated by the linear trapezoidal method.

### Theoretical

Figure 1 represents the PK–PD model governing the glucodynamics of intravenous insulin infusion in the rat. The pharmacokinetics of insulin within the plasma are described in a two-compartment open model employing Michaelis–Menten elimination kinetics, described as follows:

$$\frac{dIns_1}{dt} = K_0 - \left(k_{12} + \frac{V_{max}}{K_m + Ins_1}\right) \cdot Ins_1 + k_{21} \cdot Ins_2 \tag{1}$$

$$\frac{dIns_2}{dt} = k_{12} \cdot Ins_1 - k_{21} \cdot Ins_2 \tag{2}$$

$$C_1 = \frac{Ins_1}{V} \tag{3}$$

where $Ins_1$ is the amount of IRI within the central (plasma) compartment, and $Ins_2$ is the amount of IRI within the peripheral compartment. $K_0$ is the infusion rate (mIU $kg^{-1}$ $min^{-1}$), and $k_{12}$ and $k_{21}$ are first-order constants ($min^{-1}$) between the central and peripheral compartments. $V_{max}$ and $K_m$ (mIU $kg^{-1}$ $min^{-1}$ and mIU $kg^{-1}$) are Michaelis–Menten kinetic constants. $C_1$ is the plasma concentration (mIU $mL^{-1}$) of insulin, and V is the distribution volume (mL $kg^{-1}$) of the central compartment. Since there was a typical counter-clockwise hysteresis between the plasma IRI concentration and the plasma glucose level, an effect compartment model of Sheiner et al (1979) was introduced to the analysis of the PK–PD relationship. Briefly, in this model, the effect site is assumed to be a separate compartment which is directly connected to the central compartment by a first-order rate process ($k_{1e}$: $min^{-1}$). The elimination of IRI from the effect compartment is also characterized by a first-order rate process ($k_{e0}$: $min^{-1}$). At steady state, the influx of insulin to the effect compartment is equal to the efflux from the compartment ($Vk_{1e} = V_e k_{e0}$, where $V_e$ is the distribution volume of the effect compartment). A differential equation entailing the IRI level in the effect compartment ($C_e$: $\mu IU$ $mL^{-1}$) is described in equation 4:

$$\frac{dC_e}{dt} = k_{e0} \cdot (C_1 - C_e) \tag{4}$$

The relationship between glucodynamics and $C_e$ can be described by a sigmoid $E_{max}$ model with a baseline effect, as shown in equation 5:

$$\text{Glucodynamics} = E_0 - \frac{E_{max} \cdot C_e^\gamma}{EC50^\gamma + C_e^\gamma} \tag{5}$$

Where $E_0$ is the basal level of plasma glucose, $E_{max}$ is the maximum effect attributed to insulin, EC50 is the drug level producing 50% of $E_{max}$, and $\gamma$ is Hill's constant.
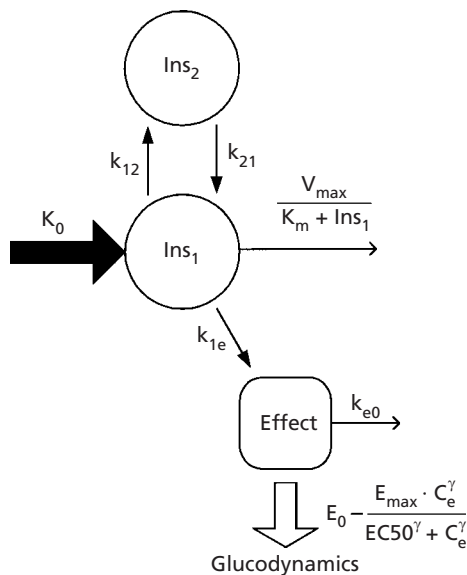
### Results

#### Conventional PK–PD analysis

Changes over time in plasma IRI concentrations after intravenous infusion of insulin (total dose levels: 0.2–5 IU $kg^{-1}$) to rats, at various infusion rates (3.3–83.3 mIU $kg^{-1}$ $min^{-1}$), are shown in Figure 2. Here, the plotted points represent the concentration of plasma IRI found at specific time intervals for each rate of infusion. During infusion, plasma IRI concentrations increased without reaching a steady state, while after infusion ended, a two-exponential decline within IRI levels was observed. Since the total clearance of IRI decreased as the dose of insulin increased (data not shown), the plasma concentrations of IRI were fitted to a two-compartment model with Michaelis–Menten type elimination kinetics, as
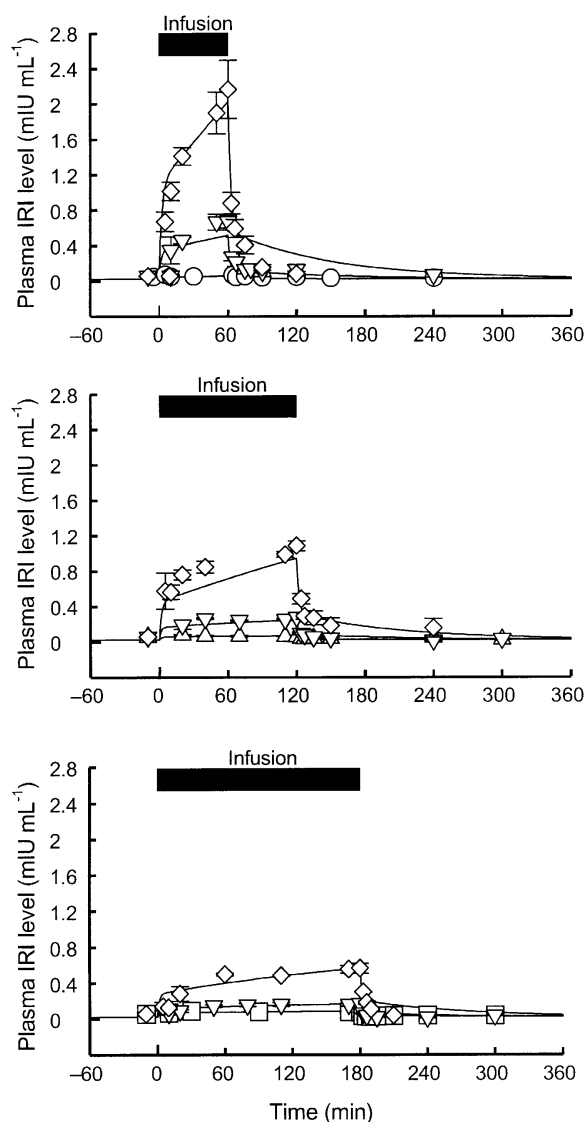


**Figure 1**  Representation of PK–PD model for hypoglycaemic effects after intravenous infusion of insulin in rats.

**Figure 2** Time courses of plasma immuno-reactive insulin (IRI) level after intravenous infusion of insulin at doses of 0.2 (○), 0.5 (△), 1 (□), 2 (▽) and 5 (◇) IU kg$^{-1}$ in rats. Points represent the mean ± s.e.m., n = 3. Solid lines represent theoretical curves according to equations 1–3.

**Table 1** Pharmacokinetic and pharmacodynamic parameters of insulin infused intravenously in rats

| Parameters | Estimates |
|---|---|
| Pharmacokinetic parameters | |
| $k_{12}$ (min$^{-1}$) | $0.337 \pm 0.015$ |
| $k_{21}$ (min$^{-1}$) | $0.016 \pm 0.001$ |
| $V_{max}$ (mIU kg$^{-1}$ min$^{-1}$) | $42.70 \pm 0.95$ |
| $K_m$ (mL kg$^{-1}$) | $134.80 \pm 2.61$ |
| V (mL kg$^{-1}$) | $134.80 \pm 2.61$ |
| Pharmacodynamic parameters | |
| $k_{e0}$ ($\times 10^{-2}$ min$^{-1}$) | $3.5 \pm 0.2$ |
| $E_0$ (mg dL$^{-1}$) | $134.2 \pm 0.7$ |
| $E_{max}$ (mg dL$^{-1}$) | $101.8 \pm 5.0$ |
| EC50 ($\mu$IU mL$^{-1}$) | $79.3 \pm 0.4$ |
| $\gamma$ | $2.6 \pm 0.3$ |

Data represents the computer-fitted value ± s.d.

shown in Figure 1. The solid lines shown in Figure 2 represent the results of the least-squares regression fitting of the intravenous infusion data to the model, and the estimated PK parameters are listed in Table 1.

Changes over time in plasma glucose levels (glucodynamics) following intravenous infusion (total dose levels: 0.5, 1, and 2 IU kg$^{-1}$), at various infusion rates (2.8–33.3 mIU kg$^{-1}$min$^{-1}$), are shown in Figures 3A–C, in which the concentration of glucose is plotted against time for each rate of infusion. The glucose level gradually

decreased after the start of infusion, and then recovered to its basal level after the end of infusion. Since there was a typical counter-clockwise hysteresis between plasma IRI levels and plasma glucose concentrations, as shown in Figures 3D–F, an effect-compartment model was applied to the PK–PD analysis (Figure 1). The solid lines, shown in Figures 3A–C, represent the results of the simultaneous fitting of the pharmacological data to the PK–PD model described in the theoretical section. The estimated PD parameters are listed in Table 1. As shown in the figures, the regression curves in slow infusion rate studies (Figures 3B and 3C) fitted the observed data well; however, the curves of the fast infusion study (Figure 3A) did not fit the observed data well. These facts indicate that the pharmacological effect of insulin is highly dependent on its infusion (input) rate.

## Input-rate-dependent PK–PD relationship

To elucidate the influence of dosing rates on the PK–PD relationship of insulin, the pharmacological data were refitted to the model for each dosing rate (Figure 4), and the estimated PD parameters were compared. The regression curves in Figure 4 trace the observed data well, particularly those involving high infusion rates. As shown in Table 2, EC50 values were significantly influenced by the infusion rate. When the infusion rate was sufficiently low (less than 10 mIU kg$^{-1}$ min$^{-1}$), the EC50 was almost constant. When the infusion rate exceeded 16 mIU kg$^{-1}$ min$^{-1}$, EC50 values increased with the infusion rate. To clarify this relationship precisely, the time course governing the pharmacological effects of insulin was determined over a wide range of infusion
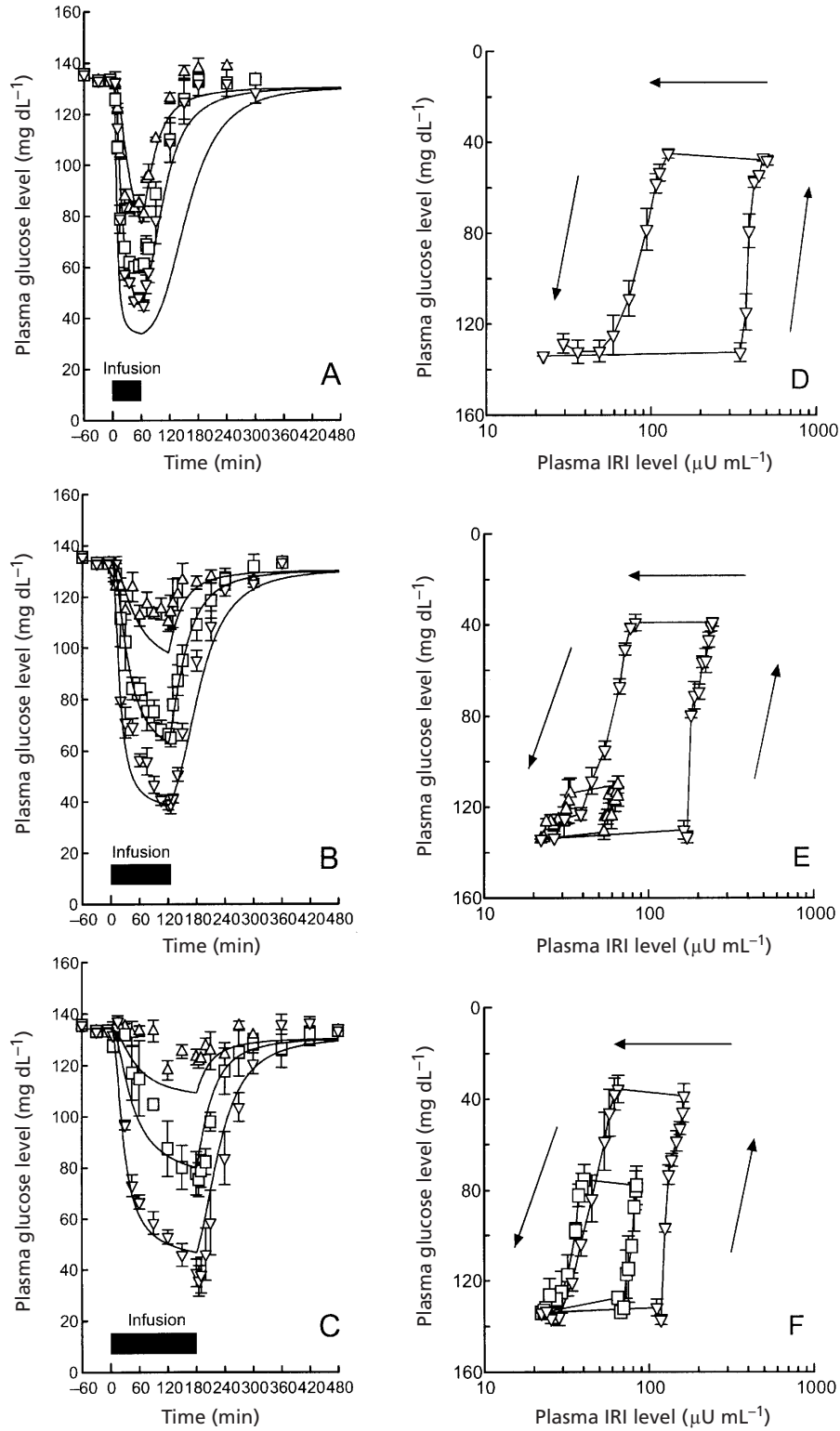
**Figure 3** Time courses of plasma glucose level (A–C), and relationship between calculated plasma immuno-reactive insulin (IRI) level and plasma glucose level (D–F) after intravenous infusion of insulin in rats. Insulin was administered at doses of 0.5 ($\triangle$), 1 ($\square$) and 2 IU kg$^{-1}$ ($\triangledown$) for 60–180 min. Each value represents the mean $\pm$ s.e.m., n = 3–4. Solid lines are theoretical curves according to equations 1–5.
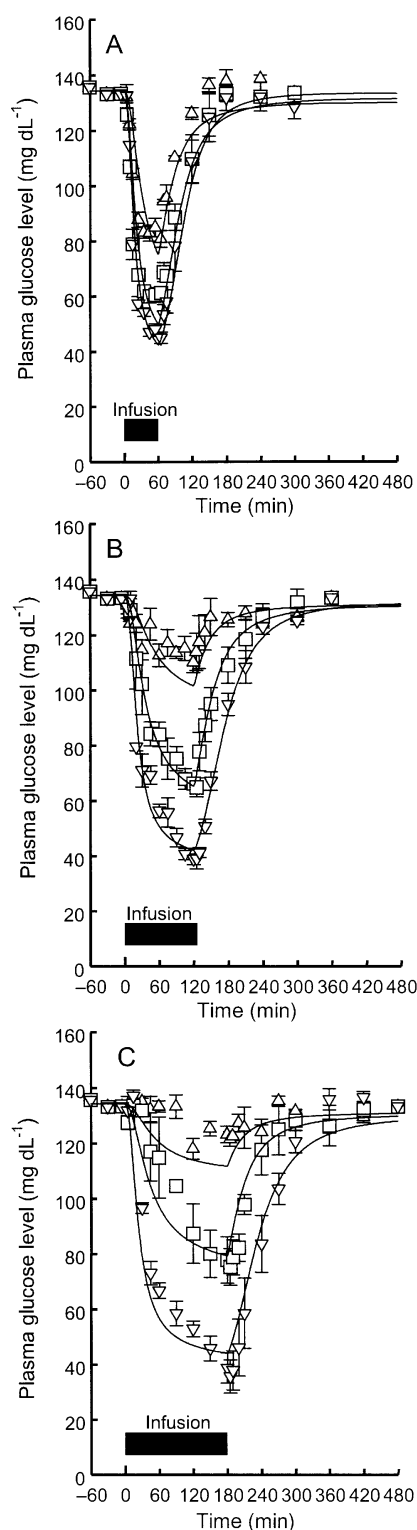
**Figure 4** Comparison of model-calculated plasma glucose level with observed data after intravenous infusion of insulin in rats. Insulin was administered at doses of 0.5 ($\triangle$), 1 ($\square$) and 2 IU kg$^{-1}$ ($\triangledown$) for 60–180 min. Each value represents the mean $\pm$ s.e.m., n = 3–4. Solid lines are theoretical curves refitted to the model for each dosing rate.

**Table 2** Estimated EC50 using glucodynamics after intravenous infusion of insulin in rats

| Infusion Rate (mIU kg$^{-1}$ min$^{-1}$) | Dose (IU kg$^{-1}$) | Period (min) | EC50 ($\mu$IU mL$^{-1}$) |
|---|---|---|---|
| 2.8 | 0.5 | 180 | 83.7 $\pm$ 3.1 |
| 4.2 | 0.5 | 120 | 84.3 $\pm$ 3.0 |
| 5.6 | 1 | 180 | 78.7 $\pm$ 4.9 |
| 8.3 | 0.5 | 60 | 77.2 $\pm$ 3.2 |
| 8.3 | 1 | 120 | 82.9 $\pm$ 4.7 |
| 11.1 | 2 | 180 | 72.6 $\pm$ 5.1 |
| 16.7 | 1 | 60 | 94.1 $\pm$ 6.2 |
| 16.7 | 2 | 120 | 95.9 $\pm$ 7.1 |
| 33.3 | 2 | 60 | 171.9 $\pm$ 13.0 |

EC50 = drug level producing 50 % of maximum effect. Data represents the computer-fitted value $\pm$ s.d.

rates (50 mIU kg$^{-1}$ min$^{-1}$ to 12 IU kg$^{-1}$ min$^{-1}$; total dose: 0.5, 1, and 2 IU kg$^{-1}$). Then, the PK–PD analysis was carried out again as described above, and PD parameters were estimated (the estimated PD parameters, other than the EC50, were comparable with the previous values). The estimated EC50 values were plotted against the logarithm of infusion rates, as shown in Figure 5A. When the infusion rate exceeded a critical value, the EC50 values began to increase log-linearly with infusion rates. EC50 values remained constant (79.3 $\mu$IU mL$^{-1}$) when the infusion rate was sufficiently slow. The results of the regression analysis indicate that the critical infusion rate is 6.97 mIU kg$^{-1}$ min$^{-1}$. In light of this, the PK–PD model was modified so as to respond to the input-rate-dependent pharmacodynamics of insulin. Then, the plasma glucose levels following a rapid infusion of insulin (50–12 000 mU kg$^{-1}$ min$^{-1}$; total dose: 0.5, 1, and 2 IU kg$^{-1}$) were re-analysed using the modified PK–PD model, and the dosing rates were estimated backward. As shown in Figure 5B, the model predicted that the calculated infusion rates were almost identical to the actual infusion rates ($r^2$ = 0.991, slope = 0.975, intercept = –1.21). Furthermore, plasma IRI levels after an extra-rapid intravenous infusion of insulin (1 and 2 IU kg$^{-1}$ for 10 s; corresponding to bolus injection) were reasonably simulated by the modified PK–PD model, as shown in Figure 6. These results indicate that the modified PK-PD model can explain the hypoglycemic effect of insulin over a wide range of doses and dosing rates.

Figure 7 represents the relationship between AUEs and the infusion rates of insulin. The solid lines show AUE values calculated from the model-predicted plas-
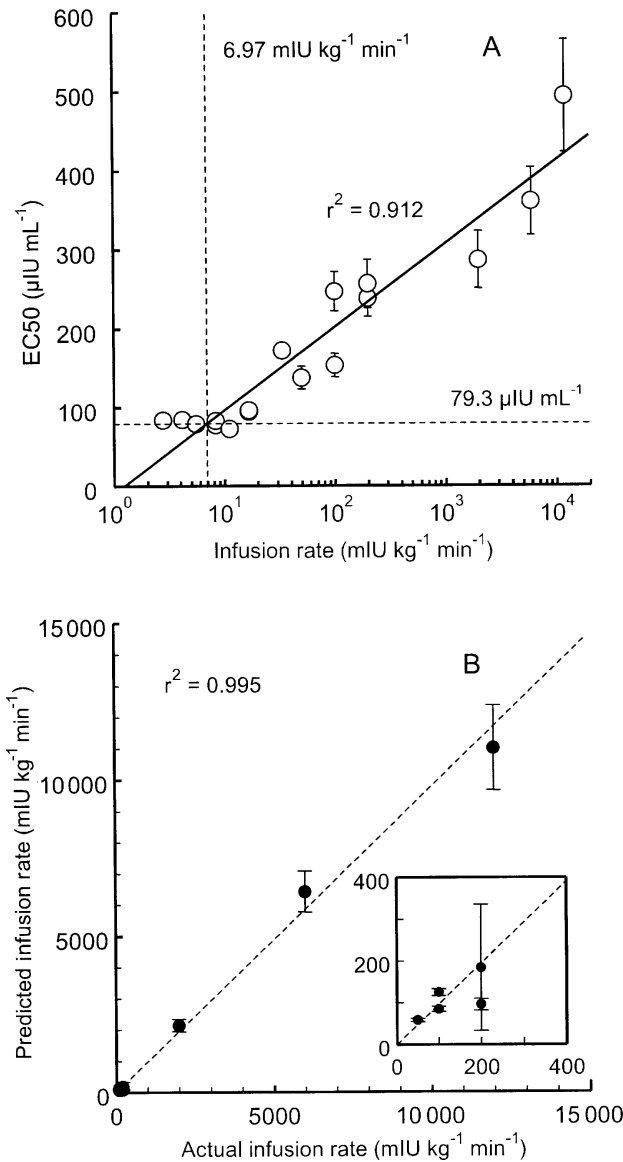
**Figure 6** Comparison of model-calculated plasma immuno-reactive (IRI) level with observed data after intravenous infusion of insulin for 10 s in rats. Insulin was administered at doses of 1 ($\bullet$) and 2 ($\blacklozenge$) IU $kg^{-1}$ for 10 s. Each value represents the mean $\pm$ s.e.m., n = 3. The solid lines are theoretical curves by the modified model.

**Figure 5** Relationship between infusion rate and EC50 (A), and comparison of model-calculated infusion rate with actual rate (B) after intravenous infusion of insulin in rats. A. Points represent the mean $\pm$ s.d., n = 3–4. The solid line represents the regression curve ($r^2 = 0.912$). B. Points represent the computer-fitted parameter $\pm$ s.d. and the dashed line represents the regression curve ($r^2 = 0.995$, slope = 0.975, intercept = –1.21).

be used as a substitute for the AUC, unless the dosing rate is sufficiently slow. The theoretical curve at the lowest dose led to a poorer prediction of observed data than those at the other doses. This may be due to a cumulative error in the observed AUE because of a slight hypoglycaemic effect at the dose.

### Prediction of the subcutaneous bioavailability

The plotted points shown in Figure 8A represent plasma glucose levels after the administration of two dosing rates of insulin via the Osmotic Mini Pump (the releasing rates used were 1.25 and 2.50 IU per day, respectively) in rats. After a lag period (about 8 h), plasma glucose levels began to decrease and then stabilized at a hypoglycaemic state for more than 48 h postdose. The apparent overshoot of hypoglycaemic effect was observed within 24 h after administration. The similar profile has been reported as a release property of this osmotic pump (Ray & Theeuwes 1987). Previously, the release rates of insulin from the Osmotic Mini Pump were determined by an in-vitro experiment. Figure 9 represents the cumulative amount of insulin released from the Osmotic Mini Pump into the isotonic phosphate buffer. The in-vitro release of insulin showed typical zero-order characteristics after a short lag period (about

ma glucose levels, and the plotting points represent the AUE values as calculated from actual glucose levels after various infusion rates of insulin. The theoretical curves described the observed data well. The AUE values gradually decrease as the logarithm of the dosing rate increases, and approaches a respective constant value. These results clearly indicate that the AUE should not
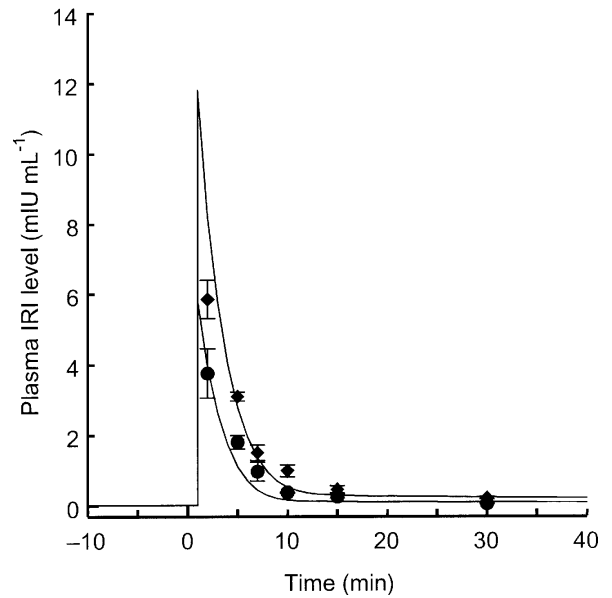
**Table 3** Comparison of model-predicted dosing rate with in-vitro data

| Releasing/Dosing rate (mIU kg$^{-1}$ min$^{-1}$) | |
| --- | --- |
| In-vitro[a] | In-vivo[b] |
| 2.31 ± 0.30 | 2.75 ± 0.51 |
| 4.41 ± 0.31 | 4.51 ± 0.47 |

[a]Calculated rate, as rat weight of 250 g, from the in-vitro releasing data. Each value is expressed as the mean ± s.d., of 3 experiments.
[b]Model-predicted rate (K$_{0s.c.}$) from the in-vivo pharmacological data. Each value is expressed as the computer-fitted value ± s.d.
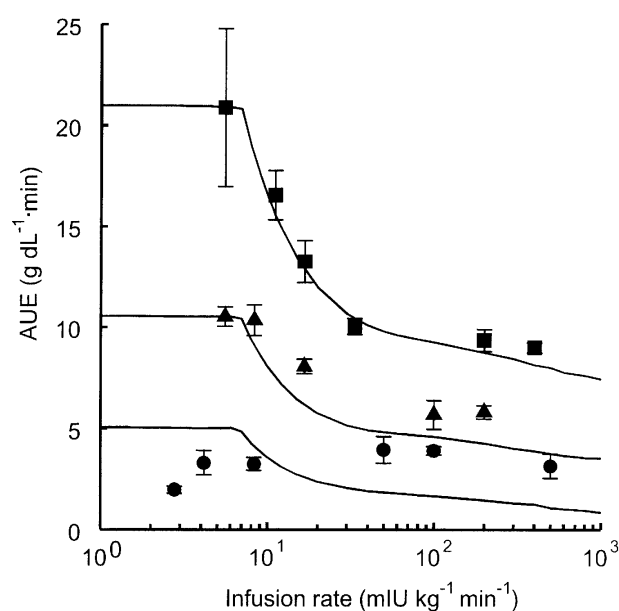


**Figure 7** Relationship between infusion rate and AUE after intravenous infusion of insulin in rats. Points represent the mean ± s.e.m., n = 3–4 at doses of 0.5 (●), 1 (▲) and 2 IU kg$^{-1}$ (■). Solid lines represent simulation curves.

8–9 h). The release rates were calculated from the slope of the straight line of the graph, using a least-squares method. The in-vitro release rates of insulin from the Osmotic Mini Pump were 0.578 ± 0.035 and 1.100 ± 0.036 mIU min$^{-1}$ (mean ± s.e.m., n = 3). If these pumps are applied to rats weighing 250 g, the dosing rates are calculated to be 2.31 and 4.41 mIU kg$^{-1}$ min$^{-1}$, respectively, as shown in Table 3, and these dosing rates are sufficiently smaller than the critical infusion rate (6.97 mIU kg$^{-1}$ min$^{-1}$).
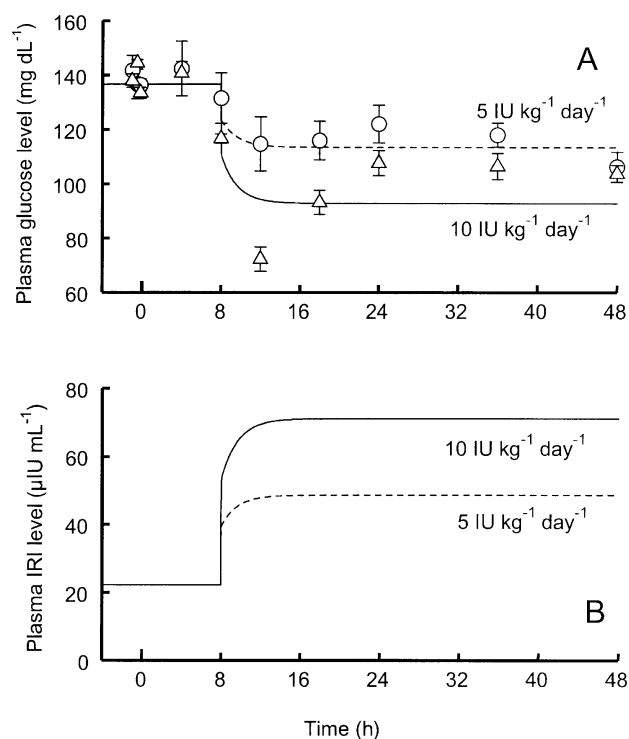


**Figure 8** Time courses of glucose (A) and immuno-reactive insulin (IRI) (B) level in plasma after subcutaneous application of the Osmotic Mini Pumps at doses of 5 and 10 IU kg$^{-1}$ in rats. Points represent the mean ± s.e.m., n = 3–5. Dashed and solid lines represent theoretical curves. Assumed pharmacokinetic and pharmacodynamic parameters are shown in Table 1.

The plasma glucose data obtained after application of the Osmotic Mini Pump was fitted to the PK–PD model shown in Figure 1, to predict the time course governing plasma IRI concentrations. Since a distinct absorptive lag time (t$_{lag}$) was observed, the time until insulin appears within the systemic circulation (t) is described as follows:

$$t = T - t_{lag} \tag{6}$$

where T is the time after the subcutaneous application of the Osmotic Mini Pump. During the pump application, insulin was continuously released according to a zero-order process. Thus, equation 1 of the model should be replaced by the following equation:

$$\frac{dIns_1}{dt} = K_{0s.c.} - \left(k_{12} + \frac{V_{max}}{K_m + Ins_1}\right) \cdot Ins_1 + k_{21} \cdot Ins_2 \tag{7}$$

where, K$_{0s.c.}$ is the release rate (mIU kg$^{-1}$ min$^{-1}$) of insulin from the Osmotic Mini Pump. Since dosing (release) rates were sufficiently smaller than the critical infusion rate (6.97 mIU kg$^{-1}$ min$^{-1}$), all of the PK and PD parameter values, including the EC50 value, were fixed to the previous values listed in Table 1. The lines
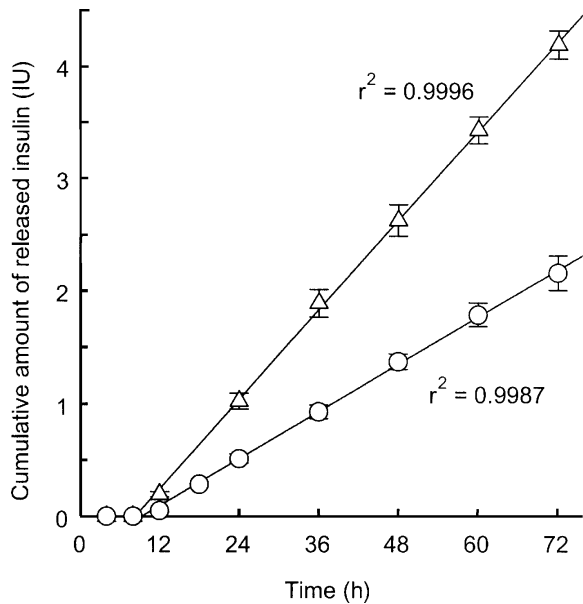
**Figure 9** In-vitro release of insulin from the Osmotic Mini Pumps incubated in isotonic phosphate buffer (pH 7.4). The theoretical release rates are 1.25 ($\bigcirc$) and 2.5 IU day$^{-1}$ ($\triangle$). Each value represents the mean $\pm$ s.em. of 3 experiments. The solid lines are the regression curves.

shown in Figure 8A represent the results of the least-squares regression fitting of the plasma glucose data to the PK–PD model (equations 2–7), and the estimated $K_{0s.c.}$ values are listed in Table 3. The lines in Figure 8A trace the observed data well, regardless of the dose administered. The estimated $K_{0s.c.}$ values are comparable with those predicted from the in-vitro release study (Table 3).

The insulin release from the Osmotic Mini Pump was continuously maintained over a 48-h period. The extent of bioavailability ($EBA_{s.c.\,(0–48\,h)}$) after subcutaneous application of the Osmotic Mini Pump, from 0–48 h, was then estimated as follows: since the solid lines shown in Figure 8B represent the model-predicted plasma IRI concentrations, $AUC_{s.c.\,(0–48\,h)}$ values were calculated using these plasma IRI values. $EBA_{s.c.\,(0–48\,h)}$ values were then estimated with the following equation:

$$EBA_{s.c.(0–48h)} = \frac{\dfrac{AUC_{s.c.(0–48h)}}{D_{s.c.}}}{\dfrac{AUC_{infusion(0–48h)}}{D_{infusion}}} \quad (8)$$

where $D_{s.c.}$ and $D_{infusion}$ are the subcutaneous dose, and the intravenous slow infusion dose, respectively. In this study, the actual $EBA_{s.c.\,(0–48\,h)}$ could not be calculated because the plasma concentrations of IRI after ap-

**Table 4** Comparison of $PA_{s.c.}$ with model-predicted $EBA_{s.c.}$ after subcutaneous administration of insulin using the Osmotic Mini Pump in rats

| Availabilities[a] (%) | Reference dose | Dose (IU kg$^{-1}$ per day) | |
| --- | --- | --- | --- |
| | | 5 | 10 |
| $EBA_{s.c.\,(0–48\,h)}$ | – | 91.64 | 95.72 |
| $PA_{s.c./bolus\,(0–48\,h)}$ | Bolus | 259.5 (283) | 311.5 (325) |
| $PA_{s.c./infusion\,(0–48\,h)}$ | Infusion | 78.48 (86) | 91.87 (96) |

[a]Derived using the data from t = 0–48 h. Data represents the mean (n = 3–4). Values in brackets represent a percentage of $EBA_{s.c.\,(0–48\,h)}$ at the corresponding dose. EBA, extent of bioavailability; PA, pharmacological availability.

plication of the Osmotic Mini Pump were below the limit of determination.

The PA after subcutaneous administration of the Osmotic Mini Pump, from 0–48 h, was calculated as below. $AUE_{s.c.\,(0–48\,h)}$ values were calculated from the model-predicted plasma glucose levels shown in Figure 8A. The PA was calculated in the following two different ways:

$$PA_{s.c./bolus(0–48h)} = \frac{\dfrac{AUE_{s.c.(0–48h)}}{D_{s.c.}}}{\dfrac{AUE_{bolus(0–48h)}}{D_{bolus}}} \quad (9)$$

$$PA_{s.c./infusion(0–48h)} = \frac{\dfrac{AUE_{s.c.(0–48h)}}{D_{s.c.}}}{\dfrac{AUE_{infusion(0–48h)}}{D_{infusion}}} \quad (10)$$

where $AUE_{bolus(0–48\,h)}$ and $AUE_{infusion(0–48\,h)}$ are the areas under the pharmacological activity versus time curves, from 0–48 h, after intravenous bolus and slow intravenous infusion, respectively. The estimated $EBA_{s.c.\,(0–48\,h)}$, $PA_{s.c./bolus(0–48\,h)}$ and $PA_{s.c./infusion\,(0–48\,h)}$ values are listed in Table 4. The PA values obtained after application of the Osmotic Mini Pump were as highly dependent on the intravascular dosing rates as the reference formulation. If the reference formulation is administered through bolus intravenous infusion, the $PA_{s.c./bolus\,(0–48\,h)}$ is approximately 3 times larger than the $EBA_{s.c.(0–48\,h)}$. However, if the reference formulation is administered by slow intravenous infusion, the $PA_{s.c./infusion\,(0–48\,h)}$ value is comparable with the $EBA_{s.c.\,(0–48\,h)}$. This indicates that PA should not be used as a substitute for EBA, unless an intravascular dosing

rate comparable with the reference formulation is available.

## Discussion

### Non-linear pharmacokinetics of insulin

Since the systemic clearance of insulin after intravenous infusion in the rat showed dose-dependent characteristics, the pharmacokinetic analysis of plasma insulin was carried out using a conventional two-compartment open model with Michaelis–Menten elimination kinetics. Saccà et al (1984) reported that the systemic clearance of insulin in man is reduced when serum concentrations are above physiological levels. The concentration-dependent elimination kinetics of insulin can be attributed to the following mechanism: after binding to the receptor, insulin is internalized and degraded within its target cells (Goldstein & Livingston 1981; Authier et al 1996). Since this process is known to be capacity-limited, the overall elimination kinetics of insulin show non-linear characteristics. Although Fugleberg et al (1982) and Morishima et al (1985) demonstrated that the kidney was not responsible for saturable insulin degradation, there is no data for non-saturable clearance of human insulin in rats. Therefore, we analysed the pharmacokinetics of insulin in rats using a conventional saturable elimination kinetics.

### PK–PD modelling for hypoglycaemic effect of insulin

Bergman et al (1979) introduced the minimal model for quantitative estimation of insulin sensitivity, and the model is widely used in physiological, pathological and epidemiological studies. It is well known that insulin exerts its pharmacological activity through binding to the membrane receptors, which exist mainly in the liver, adipose tissue and smooth muscle. Recently, studies concerning the glucoregulatory effect of insulin extend to the biochemical processes such as glucose transporter dynamics (Oatey et al 1997). Despite these reports, we constructed a conventional PK–PD model with an effect compartment, rather than a mechanism-based PK–PD model. The prime objective of this study is to assess whether the plasma IRI level is predicted accurately from plasma glucose level. The low $k_{e0}$ value in the model (Table 1, $t_{\frac{1}{2}}$ = ca. 20 min) demonstrates a slow onset of action, representing the time required for the processes, such as distribution of insulin to the receptor site, uptake of glucose by the transporter, and so on.

The amount of binding of insulin to fat cells reaches a peak within 5 min (Kono & Barham 1971). In the isolated rat cardiac myocytes, the activity of the glycogen synthesis, which is a next step after glucose uptake, was transiently increased after 5–15 min of incubation in the presence of insulin, but not after 30 min of incubation (Saeki et al 1987). In addition, the slow onset might result from the effect of hyperglycaemic factors (ex. glucagon). The increases in plasma glucagon were, however, associated with the hypoglycaemia induced by insulin (Chap et al 1987). Therefore the delay of action shown in the model for insulin may represent a synthetic rate of glucose in the regulation system of animals.

### Dosing-rate-dependent pharmacodynamics

The hypoglycaemic effect of insulin following intravenous infusion at various dosing rates cannot be described using a conventional PK–PD model with a single set of parameters. The dosing rate-dependent EC50s, shown in the results section, indicate that rat sensitivity to insulin decreases as the input rate of insulin increases. A similar result has also been shown in man (Woodworth et al 1994). It is well known that insulin exerts its pharmacological activity by binding to membrane receptors which exist primarily within the liver, the adipose tissue and smooth muscle. The dissociation constants ($K_d$) for each of these insulin receptors in the rat were found to be 0.132 nmol $L^{-1}$ (ca. 20 $\mu$IU $mL^{-1}$), 0.27 nmol $L^{-1}$ (ca. 40 $\mu$IU $mL^{-1}$) and 0.26–2.06 nmol $L^{-1}$ (39–312 $\mu$IU $mL^{-1}$), respectively (Koerker et al 1990; Torlińska et al 1998). The maximal effect of insulin is obtained when nearly 90% of the hepatocyte receptors are occupied, even though only 10% of the adipocyte receptors are occupied at this point (Torlińska et al 1998). In our rapid infusion studies, the insulin concentration in the effect compartment was estimated to be 1.1–7.3 nmol $L^{-1}$ (170–1100 $\mu$IU $mL^{-1}$). The high concentrations associated with rapid infusion might saturate the receptor with insulin. Moreover, as far as the decrease in the biological sensitivity to insulin is concerned, these properties of EC50 in this study may be similar to negative cooperativity, which is known to be an insulin-specific characteristic of the receptor. At concentrations up to 100 nmol $L^{-1}$ (15 mIU $mL^{-1}$) of insulin, dissociation from the receptor accelerated in accordance with the concentration, due to negative cooperativity between the two high-affinity binding sites in the receptor molecule (Schäffer 1994; Liu et al 1995). In our study, increasing the dosing rate, the insulin concentration in plasma will be higher to decrease the hypoglycaemic effect. Although the negative co-

operativity is generally explained under the $\gamma$ value (equation 5) of unity, the $\gamma$ value was 2.3 in this study. Our models do not represent the negative cooperativity itself, but a similar property of the biological sensitivity to insulin which was observed in both the receptor and the systemic response.

In our previous report (Miyazaki et al 2000b), the amount of arginine vasopressin, a bioactive peptide, bound to the receptors after oral administration of arginine vasopressin in rats was significantly less than that after intravenous bolus injection. Consequently, the EBA, estimated from the pharmacological effects noted after the intravenous bolus injection of arginine vasopressin, was significantly lower than the actual value. That result conflicts with this study. There have been no reports concerning the saturation kinetics or negative cooperativity of arginine vasopressin receptors, although receptor desensitization or down-regulation has been reported (Chang & Kimura 1987; Dublineau et al 1992). Therefore, the properties of drug receptors may be important considerations when a dosing-rate-dependent PK–PD relationship is expected.

### Assessment of EBA$_{s.c.}$ from pharmacological effects

The relationship between infusion (dosing) rates of insulin and AUEs is illustrated in Figure 7. According to this graph, the AUE adopts different values, even at the same dose, when the infusion rate exceeds a critical value (6.97 mIU kg$^{-1}$ min$^{-1}$). Therefore the AUE cannot be used as a substitute for the AUC, unless either the input rate, or the absorption rate, of the extravascular insulin formulation is known. Because the biological half-life of insulin following subcutaneous administration by the Osmotic Mini Pump is shown to be identical with that found after an intravenous bolus injection (Lauritzen et al 1983), we assumed that insulin was rapidly absorbed from the subcutaneous tissue. Moreover, we assumed that metabolism at the dosing site was negligible. Since the in-vitro release rate of insulin from the Osmotic Mini Pump was almost identical to the absorption rate predicted from the PK–PD analysis (Table 3), we considered the above assumptions to be appropriate. The EBA$_{s.c.}$ value obtained from the theoretical plasma concentration of insulin determined following application of the Osmotic Mini Pump (Table 4) was reasonable, although the actual EBA$_{s.c.}$ could not be estimated for analytical reasons. Since the PA can be easily estimated in a model-independent manner, it is widely used for the evaluation of formulations. In this study, the PA$_{s.c./infusion}$ value of insulin obtained from a study involving a slow intravenous infusion of insulin was almost identical with the EBA$_{s.c.}$ (Table 4); this does not, however, indicate that PA can be used as a substitute for EBA$_{s.c.}$. As expected, the curvilinear relationship between the dosing rate of insulin and the AUE (Figure 7) made it difficult to predict the EBA from the PA, or from the pharmacological data, directly.

### Conclusion

The previously used method for evaluating EBA from pharmacological data can be reasonably applied to human insulin in the rat, although this method requires a precise PK–PD model based on studies in which appropriate rates of intravascular administration are determined. While the PA can be easily obtained by a model-independent method, the use of PA as a substitute for the EBA evaluation of dosage forms is not valid. This result, together with the curvilinear correlation between AUEs and dosing rates, indicates the importance of selecting an appropriate intravascular dosing rate for the reference formulation, especially for drug formulations with slow absorption rates. Because of heterogeneous characteristics of subjects, estimating PA by a precise model will be difficult to apply to clinical studies without any modification of the model. Meanwhile, in a preclinical study conducted with new drug candidates, the increasing demand for shorter cycle time in drug and its formulation selection. Thus, the approach may be a useful tool in a discovery phase; once a PK–PD model is determined for the drug level and the targeted pharmacological effect, the EBA and PA of the potential formulation will be easily and routinely predicted using only the input rate without further animal experiments.

### References

Authier, F., Posner, B. I., Bergeron, J. J. (1996) Insulin-degrading enzyme. *Clin. Invest. Med.* **19**: 149–160

Bergman, R. N., Ider, Y. Z., Bowden C. R., Cobelli, C. (1979) Quantitative estimation of insulin sensitivity. *Am. J. Physiol.* **236**: E667–E677

Chang, P., Kimura, K. (1987) Desensitization of renal vasopressin-stimulated adenylate cyclase by a vasopressor and antidiuretic antagonist, [1-($\beta$-mercapto-$\beta$, $\beta$-cyclopentamethylenepropionic acid), 2-(O-ethyl)-D-tyrosine, 4-valine] arginine vasopressin. *Biochem. Biophys. Res. Commun.* **144**: 770–778

Chap, Z., Ishida, T., Chou, J., Hartley, C. J., Entman, M. L., Brandenburg, D., Jones, R. H., Field J. B. (1987) First-pass hepatic extraction and metabolic effects of insulin and insulin analogues. *Am. J. Physiol.* **252**: E209–E217

Derendorf, H. (1994) Pharmacodynamic aspects of systemic drug delivery. *Drug Dev. Ind. Pharm.* **20**: 485–502

Dublineau, I., Pradelles, P., de Rouffignac, C., Elalouf, J.-M. (1992) Desensitization to vasopressin action in the rat kidney medulla: studies on isolated nephron segments. *Ren. Physiol. Biochem.* **15**: 57–65

Fugleberg, S., Kølendorf, K., Thorsteinsson, B., Bliddal, H., Lund, B., Bojsen, F. (1982) The relationship between plasma concentration and plasma disappearance rate of immunoreactive insulin in normal subjects. *Diabetologia* **22**: 437–440

Goldstein, B. J., Livingston, J. N. (1981) Insulin degradation by insulin target cells. *Metabolism* **30**: 825–835

Hochhaus, G., Derendorf, H. (1995) Dose optimization based on pharmacokinetic-pharmacodynamic modeling. In: Derendorf, H., Hochhaus, G. (eds) *Handbook of pharmacokinetic/pharmacodynamic correlation.* CRC Press Inc., Boca Raton, pp 79–120

Koerker, D. J., Sweet, I. R., Baskin, D. G. (1990) Insulin binding to individual rat skeletal muscles. *Am. J. Physiol.* **259**: E517–E523

Kono, T., Barham, F. W. (1971) The relationship between the insulin-binding capacity of fat cells and the cellular response to insulin. *J. Biol. Chem.* **246**: 6210–6216

Lauritzen, T., Pramming, S., Deckert, T., Binder, C. (1983) Pharmacokinetics of continuous subcutaneous insulin infusion. *Diabetologia* **24**: 326–329

Liu, R., Zhu, J., Jospe, N., Furlanetto, R. W., Bastian, W., Livingston, J. N. (1995) Deletion of lysine 121 creates a temperature-sensitive alteration in insulin binding by the insulin receptor. *J. Biol. Chem.* **270**: 476–482

Lu, W., Endoh, M., Katayama, K., Kakemi, M., Koizumi, T. (1987) Pharmacokinetic and pharmacodynamic studies of piretanide in rabbits. I. Effect of different hydrated conditions. *J. Pharmacobio-Dyn.* **10**: 356–363

Miyazaki, M., Maekawa, C., Iwanaga, K., Morimoto, K., Kakemi, M. (2000a) Bioavailability assessment of disopyramide using pharmacokinetic-pharmacodynamic (PK-PD) modeling in the rat. *Biol. Pharm. Bull.* **23**: 1363–1369

Miyazaki, M., Sawada, S., Nishide, T., Iwanaga, K., Morimoto, K., Kakemi, M. (2000b) Bioavailability assessment of arginine-vaso-pressin (AVP) using pharmacokinetic-pharmacodynamic (PK-PD) modeling in the rat. *Biol. Pharm. Bull.* **23**: 87–96

Morishima, T., Bradshaw, C., Radziuk, J. (1985) Measurement using tracers of steady-state turnover and metabolic clearance of insulin in dogs. *Am. J. Physiol.* **248**: E203–E208

Oatey, P. B., Van Weering, D. H. J., Dobson, S. P., Gould, G. W., Tavare, J. M. (1997) GLUT4 vesicle dynamics in living 3T3 L1 adipocytes visualized with green-fluorescent protein. *Biochem. J.* **327**: 637–642

Ray, N., Theeuwes, F. (1987) Implantable osmotically powered drug delivery systems. In: Johnson, P., Lloyd-Jones, J. G. (eds) *Drug Delivery Systems: Fundamentals and Techniques.* Ellis Horwood, Chichester and VCH Verlagsgesellschaft, Weinheim, pp 122–138

Saccà, L., Orofino, A., Petrone, A., Vigorito, C. (1984) Direct assessment of splanchnic uptake and metabolic effects of human and porcine insulin. *J. Clin. Endocrinol. Metab.* **59**: 191–196

Saeki, Y., Kashiwagi, A., Uehara, N. (1987) Effect of insulin on the glucose utilization in isolated cardiac myocytes from adult rat. *J. Biochem.* **101**: 977–985

Schäffer, L. (1994) A model for insulin binding to the insulin receptor. *Eur. J. Biochem.* **221**: 1127–1132

Sheiner, L. B., Stanski, D. R., Vozeh, S., Miller, R. D., Ham, J. (1979) Simultaneous modeling of pharmacokinetics and pharmacodynamics: application to *d*-tubocurarine. *Clin. Pharmacol. Ther.* **25**: 358–371

Tachibana, K. (1992) Transdermal delivery of insulin to alloxan-diabetic rabbits by ultrasound exposure. *Pharm. Res.* **9**: 952–954

Torlińska, T., Maćkowiak, P., Nogowski, L., Nowak, K. W., Madry, E., Perz, M. (1998) Characteristics of insulin receptor binding to various rat tissues. *J. Physiol. Pharmacol.* **49**: 261–270

Wald, J. A., Salazar, D. E., Cheng, H., Jusko, W. J. (1991) Two-compartment basophil cell trafficking model for methylpred-nisolone pharmacodynamics. *J. Pharmacokinet. Biopharm.* **19**: 521–536

Woodworth, J. R., Howey, D. C., Bowsher, R. R. (1994) Establishment of time-action profiles for regular and NPH insulin using pharmacodynamic modeling. *Diabetes Care* **17**: 64–69